

Sheet Beam Klystron Instability Analysis*

K.L.F. Bane, A. Jensen, Z. Li, G. Stupakov, C. Adolphsen, SLAC, Stanford, CA 94309

*Presented at the Particle Accelerator Conference (PAC 09),
Vancouver, BC, Canada, May 4-8, 2009*

*Work supported by Department of Energy contract DE-AC02-76SF00515.

SHEET BEAM KLYSTRON INSTABILITY ANALYSIS *

K.L.F. Bane, A. Jensen, Z. Li, G. Stupakov, C. Adolphsen, SLAC, Stanford, CA 94309, USA

Abstract

Using the principle of energy balance we develop a 2D theory for calculating growth rates of instability in a two-cavity model of a sheet beam klystron. An important ingredient is a TE-like mode in the gap that also gives a longitudinal kick to the beam. When compared with a self-consistent particle-in-cell calculation, with sheet beam klystron-type parameters, agreement is quite good up to half the design current, 65 A; at full current, however, other, current-dependent effects come in and the results deviate significantly.

INTRODUCTION

The development of sheet beam klystrons (SBK) for accelerator applications has been an ongoing area of research at SLAC National Accelerator Center for over a decade. The most recent developments have been for an L-band device capable of generating greater than 10 MW of RF power and an efficiency of over 70%. The beam stick (the klystron but without cavities) has been fully simulated and designed and should produce hot test results sometime soon. The beam transport is calculated using the particle-in-cell (PIC) code MAGIC3D [1], a MagNet 3D simulation of the PPM structure, and a beam imported from a 3D MICHELLE simulation of the gun.

Significant amount of calculation has also been completed for the full power 7-cavity sheet beam klystron. 1D and 2D RF simulations both predict the SBK will meet specifications. Final validation of the design with RF was attempted in 3D simulation. However, instabilities were observed as is shown in Fig. 1.

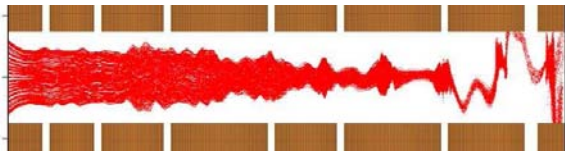


Figure 1: Magic3D simulation of a 7-cavity (at the white stripes) SBK in longitudinal view, showing an instability, with beam impinging on the walls. The sheet beam is seen from its narrow side in red; it moves from left to right.

In this report, to analyze the instability we will employ a simplified, 2D two-cavity model of the SBK. Note that some kind of analysis of a similar SBK instability has been performed by Yu and Wilson [2]. At the end we will compare results of three calculation methods: the first two—the *analytical* and *numerical* methods—both employ an energy balance equation to obtain growth rates of instability; the third is the self-consistent PIC method of MAGIC.

* Work supported by the DOE contract DE-AC02-76SF00515.

The 2D two-cavity model that will be used in the calculations is sketched in Fig. 2. The length of the gap—the separation between the two cavities—is denoted by l , and the beam-pipe height by h . The width of the gap in the klystron, w , is much larger than the height, thus justifying the 2D approximation. The nominal beam kinetic energy $\mathcal{E}_k = 115$ keV and the beam current, $I = 130$ A. Important beam and structure parameters are collected in Table 1. In this report we will work in Gaussian units.

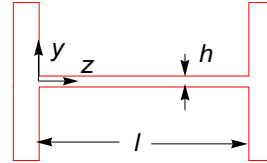


Figure 2: 2D two-cavity model used for the calculations.

Table 1: Parameters used in the simulations.

Parameter	Value	Units
Beam Kinetic Energy, \mathcal{E}_k	115.	keV
Beam Current, I	130.	A
Ratio V_z'/E_0	0.67	
Length of gap, l	133.5	mm
Height of gap, h	7.5	mm
Width of gap, w^*	145	mm

THEORY

The instability mechanism can be described qualitatively as follows: Let us suppose there is a TE-like mode present in the gap. A part of the beam enters the gap on axis with zero slope, and through the transverse fields it will arrive at the end of the gap off axis. The mode has non-zero longitudinal electric field near the end of the gap that depends on vertical position (it is zero on axis). Depending on the phase of the beam part of interest, the beam either puts energy into the mode or takes energy out of it through this field. If, when averaging over the entire beam, the net effect is to put energy into the mode, then the beam will drive the mode to larger amplitudes and there is instability.

For our analysis we let the $+z$ -axis follow the symmetry line of the beam pipe to the right in Fig. 2 (with $z = 0$ at the beginning of the gap), $+y$ is in the vertical direction, and $+x$ points into the plane. The amplitudes of the non-zero field components E_y , E_z , and B_x of the TE₁₁-like mode in the 2D structure were obtained using SUPERFISH and are given in Fig. 3. Note that (i) the overall scale factor of the fields is not important and does not factor into our

*Ours is a two-dimensional model, and we cannot distinguish the beam width from the gap width.

final result, (ii) E_z is zero on axis and varies linearly with small offset (in our case an offset of $y_0 = 1$ mm was used), and (iii) electric field is 90° out of phase with the magnetic field. For our *analytical* calculations we use sinusoidal approximations to E_y and B_x (the dashed curves in the plot), and replace E_z with a delta-function voltage kick at the end of the gap. That is, the transverse fields are given by

$$\begin{aligned} E_y &= E_0 \cos(\omega t) \cos(\omega z/c), \\ B_x &= -E_0 \sin(\omega t) \sin(\omega z/c), \end{aligned} \quad (1)$$

where t is time, $\omega = \pi c/l = 7.63 \times 10^9$ /s is the frequency of the mode, and c is the speed of light.

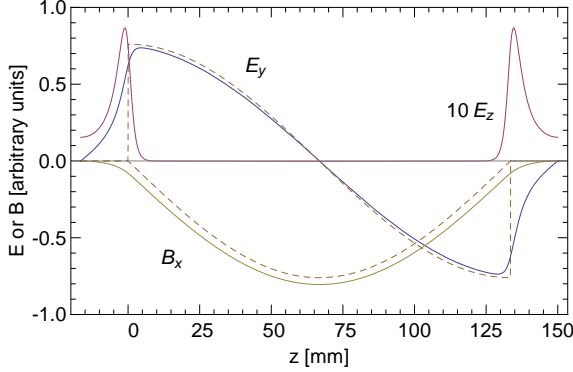


Figure 3: Fields in the 2D, 2-cavity model (solid), and the sinusoidal approximations of E_y and B_x (dashes).

Let us now consider a particle that enters the gap at time $t = \tau$, and moves at velocity v_0 in the $+z$ direction (for a beam energy of 115 keV, $v_0 = 0.58c$). The voltage kick it experiences at the end of the gap, for small y , is

$$FV_z(y) \cos(\omega t + \psi) \approx FV'_z y \cos(\omega t + \psi), \quad (2)$$

where $V'_z = (dV_z/dy)|_{y=0} \approx (\int E_z dz)/y_0$, where the integral over E_z is taken over the downstream spike (see Fig. 3); where the phase ψ and factor F are given by

$$\begin{aligned} \begin{bmatrix} c_1 \\ c_2 \end{bmatrix} &= \int E_z(z) \begin{bmatrix} \sin[\frac{\omega}{v_0}(z-l)] \\ \cos[\frac{\omega}{v_0}(z-l)] \end{bmatrix} dz, \\ \psi &= \tan^{-1}(c_1/c_2), \quad F = \sqrt{c_1^2 + c_2^2} / \int E_z dz. \end{aligned} \quad (3)$$

We assume that the mode amplitude E_0 is small, of the first order. The transverse field of the mode will deflect the particle in the y direction. In addition to the fields of the mode, there is also a focusing magnetic field, which we approximate as a smooth focusing channel with betatron frequency of oscillation ω_β . The transverse motion of the particle is governed by the equation

$$\frac{d^2}{dt^2} Y(t) + \omega_\beta^2 Y(t) = \frac{e}{m\gamma} \left(E_y + \frac{v_0}{c} B_x \right), \quad (4)$$

where e is charge and m is mass of the electron, and γ is the Lorentz energy factor. The z coordinate of the particle

is given by $z = v_0(t - \tau)$ (we take v_0 to be fixed), so Eq. 4 can be considered an equation of time only. Note that for our *numerical* results we numerically integrate Eq. 4 using the numerical fields shown in Fig. 3.

For initial conditions, we assume the electron enters the gap on axis with zero slope, *i.e.* $Y(\tau) = Y'(\tau) = 0$. Then the solution to Eq. (4) is $Y(t) = \text{Re} \tilde{Y}(t)$, with

$$\begin{aligned} \tilde{Y}(t) &= \sum_{n=1}^2 \frac{A_n e^{(-1)^{n+1} i\phi + i\Omega_n \tau}}{\omega_\beta^2 - \Omega_n^2} \left[e^{i\Omega_n(t-\tau)} \right. \\ &\quad \left. - \cos(\omega_\beta[t - \tau]) - i \frac{\Omega_n}{\omega_\beta} \sin(\omega_\beta[t - \tau]) \right], \end{aligned}$$

$$A_n = \frac{eE_0}{2m\gamma} [1 + (-1)^n \beta], \quad \Omega_n = \omega [1 + (-1)^n \beta]; \quad (5)$$

$\phi = \omega\tau\beta$ and $\beta = v_0/c$.

We now need to calculate the energy balance between the mode and the particles. The energy \mathcal{E} that a particle gains (or loses) is caused by the longitudinal field in the mode at the exit of the gap and by the vertical field throughout the gap. The first contribution can be calculated using Eq. (2) where y is substituted by the function Y taken at exit time $T = \tau + l/v_0$:

$$\mathcal{E}_1 = eFV'_z Y(T) \cos(\omega T + \psi), \quad (6)$$

and the second piece is given by

$$\mathcal{E}_2 = e \int_{\tau}^T E_y(t) \frac{d}{dt} Y(t) dt. \quad (7)$$

Since we have a constant stream of particles that arrive at different times τ , these equations must be averaged over τ . The result is $\langle \mathcal{E} \rangle = \langle \mathcal{E}_1 + \mathcal{E}_2 \rangle$ ($\langle \rangle$ means to average over τ), and

$$\langle \mathcal{E} \rangle = - \frac{e^2 l^2}{2\pi^2 m c^2} E_0^2 G(\alpha, \beta), \quad (8)$$

where $\alpha = \omega_\beta/\omega$ and G is an analytical function with many terms (that we do not show here). If $\langle \mathcal{E} \rangle$ is positive, then, on average, the beam takes energy from the mode, and the mode damps; if it is negative, then the beam deposits energy into the mode, and the mode can grow. Note that since the beam cannot lose energy to the transverse field (it initially has no energy in transverse motion), the $\langle \mathcal{E}_2 \rangle$ contribution can only damp the instability.

We finally multiply $\langle \mathcal{E} \rangle$ by the number of particles entering the gap per unit time per unit width in x , I/we (w the width of the beam), and divide it by the electromagnetic energy in the mode W (also per unit width in x), $W = E_0^2 l h / (16\pi)$. The growth rate in energy of the instability Γ is then

$$\Gamma \approx - \frac{I}{we} \frac{\langle \mathcal{E} \rangle}{W} - \frac{\omega}{Q}, \quad (9)$$

where we have introduced the quality factor of the mode Q . The first term in the above equation can be written as

$$\Gamma = - \frac{8}{\pi} \frac{cl}{wh} \frac{I}{I_A} G(\alpha, \beta), \quad (10)$$

with $I_A = 17$ kA, the Alfvén current.

Finally we should point out two conditions that need to be satisfied for the validity of our energy balance approach: (i) $|\Gamma| \ll \omega$; we shall see (in the following section) that, at full current, $|\Gamma| \sim 1 \text{ ns}^{-1}$, and since $\omega = 7.6 \text{ ns}^{-1}$ this condition will be reasonably well satisfied. (ii) A particle's transit time across the gap, Δt_l , needs to be small compared to $1/|\Gamma|$; for $\mathcal{E}_k = 115 \text{ keV}$, $\Delta t_l = 0.7 \text{ ns}$ which is comparable to $1/|\Gamma| \sim 1 \text{ ns}$. The second condition not being well satisfied may lead to error in the results.

CALCULATIONS

We begin by calculating the growth rate, for the case of no focusing, as function of beam energy at the nominal 130 A beam current. We present the results for the analytical and numerical calculations in Fig. 4 (in all our calculations we let $Q = \infty$). We see that there is good agreement between the curves. For beam energies above $\sim 35 \text{ keV}$, $\Gamma < 0$ and the beam is stable. At the nominal 115 keV the damping rate is $-\Gamma = 1 \text{ ns}^{-1}$.

In Fig. 4 we also give results of MAGIC2D, where we have used a 10 A beam but normalized the growth rate to 130 A. At higher currents, without focusing, it was difficult to calculate the growth rate because the beam tends to quickly hit the beam pipe wall. In our calculations, to obtain a clear signal of the desired mode, the structure was first preloaded with the fields of the TE_{11} -like mode at low level; then Γ was obtained from the e-folding rate of the fields. We see that there is good agreement with the energy balance calculations.

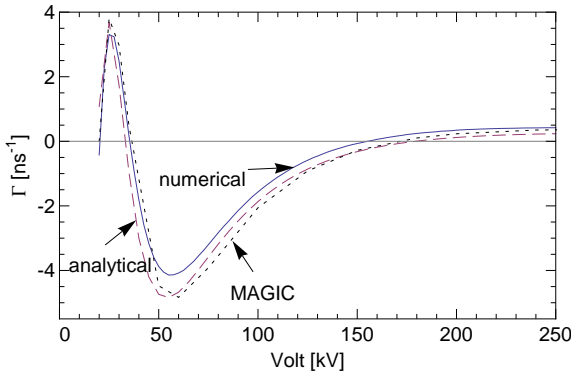


Figure 4: Growth rate—in energy—as function of beam energy in the case of no external focusing. Shown are the analytical, numerical, and MAGIC results.

For focusing the SBK beam, both solenoidal and permanent magnet (PPM) focusing have been considered. In the case of PPM focusing the magnetic field can be written as

$$B_y = -B_0 \sinh ky \cos kz, \quad B_z = B_0 \cosh ky \sin kz$$

with $B_x = 0$ and $k = 0.08 \text{ mm}^{-1}$. For our 115 keV beam, for up to $B_0 = 1 \text{ kG}$, the parameter $\alpha = \omega_\beta/\omega$ is approximately proportional to the strength of B in both PPM

and solenoid cases, with $\alpha = 1.4(B_0)_{PPM} = 1.9(B_0)_{sol}$, with B in [kG]. Note that if *e.g.* $(B_z)_{sol} = 400 \text{ G}$, then $\omega_\beta = 5.8 \text{ ns}^{-1}$. In Fig. 5 we plot, for $\mathcal{E}_k = 115 \text{ keV}$, the growth rate as function of focusing field B_z , for the analytical and numerical calculations (again at $I = 130 \text{ A}$). We see that the beam oscillates with B_z and is stable over most of the range of the plot, and that the analytical and numerical results agree well.

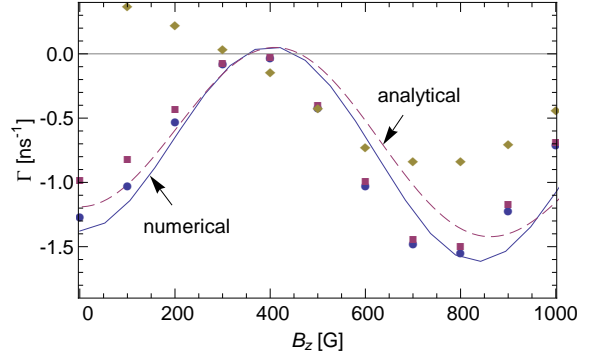


Figure 5: Growth rate—in energy—as function of focusing strength, when the beam energy is 115 keV. Shown are results of the analytical and numerical methods (the lines); also of MAGIC2D with solenoidal focusing, for $I = 10 \text{ A}$ (circles), 65 A (squares), and 130 A (diamonds), all normalized to 130 A.

In Fig. 5 we show, in addition, MAGIC2D (with solenoidal focusing) results, for beam currents $I = 10 \text{ A}$, 65 A, 130 A—all normalized to 130 A (the plotting symbols). At 10 A and 65 A, the results agree reasonably well with the energy balance calculations. The slight apparent shift with respect to the curves may be because the MAGIC simulations used dimensions that were slightly different. At 130 A the system is less stable, and is, in fact, unstable for $B_z \lesssim 300 \text{ G}$. The change we see at this current suggests that current dependent effects that were not included in our model, *e.g.* space charge, have become important.

In a SBK other modes are present and the geometry is, in fact, three dimensional. At least the *numerical* version of the energy balance calculations can be easily extended to include these effects. Including current dependent effects, such as space charge, or allowing for growth times that are short compared to the transit time will be more difficult. Nevertheless, these first calculations suggest that energy balance-type of calculations—which are quick to perform—may become useful aids in designing full sheet beam klystrons in the future.

REFERENCES

- [1] MAGIC User's Manual, Mission Research Corporation, MRC/WDC-R-409, 1997.
- [2] D. Yu and P. Wilson, in Proc. Part. Accel. Conf. (PAC93), 1993, p. 2681.